Title: Physical properties of lead-free BaFe1/2Nb1/2O3 ceramics obtained from mechanochemically synthesized powders

Author: Dariusz Bochenek, Przemysław Niemiec, Małgorzata Adamczyk, I. Szafraniak-Wiza

Citation style: Bochenek Dariusz, Niemiec Przemysław, Adamczyk Małgorzata, Szafraniak-Wiza I. (2018). Physical properties of lead-free BaFe1/2Nb1/2O3 ceramics obtained from mechanochemically synthesized powders. "Journal of Materials Science" (Vol. 53, no. 19 (2018), s. 13501-13512), doi 10.1007/s10853-018-2254-z

UNIWERSYTET ŚLĄSKI W KATOWICACH
Biblioteka Uniwersytetu Śląskiego
Ministerstwo Nauki i Szkolnictwa Wyższego

Mechanochemical Synthesis

CrossMark

Physical properties of lead-free $BaFe_{1/2}Nb_{1/2}O_3$ ceramics obtained from mechanochemically synthesized powders

D. Bochenek[1,*] (ID), P. Niemiec[1] (ID), M. Adamczyk[1] (ID), and I. Szafraniak-Wiza[2] (ID)

[1] Faculty of Computer Science and Materials Science, Institute of Technology and Mechatronics, University of Silesia in Katowice, 12 Żytnia St., 41-200 Sosnowiec, Poland
[2] Faculty of Mechanical Engineering and Management, Institute of Materials Science and Engineering, Poznań University of Technology, Jana Pawła II 24, 61-138 Poznań, Poland

ABSTRACT

Modern electronics expect functional materials that are eco-friendly and are obtained with lower energy consumption technological processes. The multiferroic lead-free $BaFe_{1/2}Nb_{1/2}O_3$ (BFN) ceramic powder has been prepared by mechanochemical synthesis from simple oxides at room temperature. The development of the synthesis has been monitored by XRD and SEM investigations, after different milling periods. The obtained powders contain large agglomerates built by crystals with an estimated size about 12–20 nm depending on the period of milling. From this powder, the multiferroic BFN ceramic samples have been prepared by uniaxial pressing and subsequent sintering pressureless method. The morphology of the BFN ceramic samples strongly depends on high-energy milling duration. The properties of the ceramic samples have been investigated by dielectric spectroscopy, in broad temperature and frequency ranges. The high-energy milling of the powders has strongly affected the dielectric permittivity and dielectric loss of the $BaFe_{1/2}Nb_{1/2}O_3$ ceramic samples. The usage of the mechanochemical synthesis to obtain the multiferroic lead-free BFN materials reduces the required thermal treatment and simultaneously improves the parameters of the BFN ceramics.

Introduction

Multiferroic materials show simultaneously at least two types of ferroic properties, i.e., a ferromagnetic (antiferromagnetic, ferrimagnetic) state, a ferroelectric (antiferroelectric, ferrielectric) state or a ferroelastic (ferromagneticelastic, ferroelastoelectric) state [1, 2]. Due to the coupling between magnetic and polarization orders, multiferroics offer wide and functional properties for applications in modern microelectronics and micromechatronics [3–6]. The largest groups of materials with these properties are

---

Springer

materials with a perovskite structure. Generally, perovskite ceramics (the best materials for smart structures, sensors and actuators) are fabricated by solid-state reactions or wet-chemistry methods [7–10]. The methods are related to high production costs and have serious disadvantages (e.g., high-temperature treatment during the technological process results in coarsening and aggregation of the particles or non-stoichiometric composition or non-perovskite structure of the final materials due to the appearance of the volatile element out-diffusion at high temperature). A much less expensive alternative to those techniques is a direct synthesis from respective oxides at room temperature, via mechanochemical reaction [11–13]. The room-temperature synthesis lowers fabrication costs, eliminates the undesirable losses of volatile elements and enables the control of chemical and stoichiometry composition.

The development of lead-free electroceramics, capable of replacing the most commonly used PZT-based materials, is currently a very important issue due to environmental considerations. One of the possible candidates to replace the lead-contained ceramics is $BaFe_{1/2}Nb_{1/2}O_3$ (BFN) material with multiferroic properties [14–17].

Recently, we have prepared and investigated the BFN ceramics obtained from mechanically activated powders [13]. The conventional process of ceramic preparation was modified by the mechanochemical activation of starting reagents (including carbonates). Usually, mechanochemical methods based on carbonates reagents require additional thermal treatment to initiate reaction. A different possibility is to use simple oxides as starting reagents, and this method usually allows a synthesis directly during high-energy milling. This paper focuses on the preparation of BFN ceramics thereby (from simple oxides) and the investigations of the influence of high-energy milling time on the final properties of ceramics. The development of the synthesis has been monitored by XRD and SEM investigations after different milling periods. The ceramic properties have been investigated by dielectric spectroscopy in broad temperature and frequency ranges. The influence of high-energy milling on the final properties of the BFN ceramics has been discussed.

Experimental details

The multiferroic lead-free $Ba(Fe_{1/2}Nb_{1/2})O_3$ (BFN) ceramics have been obtained from simple oxides by mechanochemical synthesis. The stoichiometric mixture of the starting oxides BaO (99.99% Sigma-Aldrich), Fe_2O_3 (99%, Sigma-Aldrich) and Nb_2O_5, (99.9%, Sigma-Aldrich) was placed in a stainless steel reaction vessel together with stainless steel balls. The mechanical synthesis was carried out in a SPEX 8000 Mixer Mill (shaker type mill with vial clamp speed of 875 cycles per minute) in the air atmosphere and at room temperature. The ball-to-powder weight ratio (BPR) parameter was 5:1. The high-energy mill was run for different periods between 1 and 75 h. The synthesis process was controlled by X-ray diffraction studies after various milling time. XRD measurements were performed with PANalytical Empyrean X-ray powder diffractometer (CuKα radiation, 45 kV, 40 mA). The morphology of the obtained powders samples has been examined with a scanning electron microscope (SEM) JEOL JSM-7100 TTL LV Field Emission Scanning Electron Microscope.

The mechanochemically synthesized powders have been used for the preparation of ceramic samples. The powder has been uniaxially pressed into disks with the diameter of 8 mm and thickness about 3 mm, with the usage of polyvinyl alcohol as a binder. The compacting (densification) of the BFN ceramic samples was made by a free sintering method under the following conditions: $T_s = 1350$ °C, $t_s = 4$ h (according to the previous works [13, 15]).

The SEM morphology of the fracture of the ceramic samples was carried out by a JEOL JSM-7100 TTL LV Field Emission Scanning Electron Microscope. For the electrical investigation, the ceramic specimens were ground and polished and successively silver paste electrodes (P-120 supplier Polish State Mint) have been deposited on both surfaces of the specimens. Dielectric permittivity and dielectric loss were measured during heating (between 20 and 450 °C, heating rate 1 K/min) using the capacity bridge of a QuadTech 1920 Precision LCR Meter and in the frequency range from 1 to 100 kHz. The measurements of DC electric conductivity were performed using a 6517B Keithley electrometer in the temperature range from 20 to 400 °C.

Results and discussion

The properties of multiferroic materials are closely related to their technologic processes that usually have huge impact on material crystallographic structure and microstructure. Mechanochemical synthesis offers the formation of perovskite phase directly at room temperature and fine grain powder which can be very suitable for the preparation of dense ceramic samples. Among many preparation parameters, milling time plays a very important role (e.g., milling time can determine crystalline or amorphous nature of final materials). In order to monitor the synthesis process, the oxide mixture has been milled for different times up to 75 h. After each high-energy milling period, the material has been examined by XRD measurements (Fig. 1) and SEM observations (Fig. 2).

Initially, the starting powders were mixed together and their crystallographic structures gradually disappeared as a result of high-energy milling. On the diffraction patterns, the diffraction peaks of the starting materials have been greatly broadened and their intensity decreased. The longer high-energy milling duration has triggered the synthesis process and led to a gradual appearance of the crystallographic BFN structure. After 2 h of milling, the formation of BFN perovskite phase has been evidenced due to a few XRD peaks. However, the detected perovskite peaks are weak and revealed small amounts of this new phase. During longer milling up 20 h, the amount of the perovskite phase gradually increased and the diffraction peaks become more
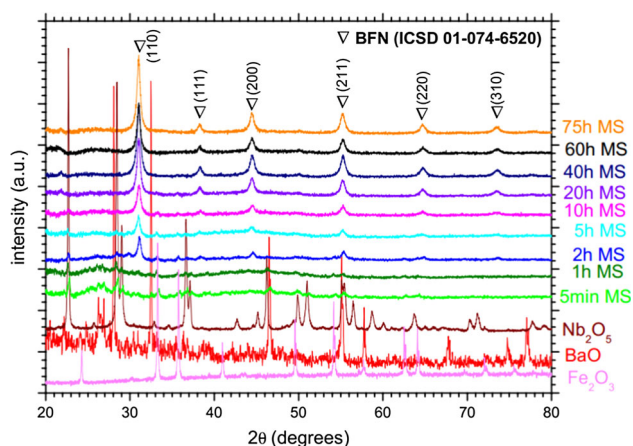
clearly visible, whereas their intensities increased. No significant difference was found for prolonged milling. The XRD patterns have revealed several relatively sharp peaks assigned to the perovskite phase; however, relatively larger background of the diffraction patterns has suggested the presence of amorphous materials. For longer milling periods (more than 50 h), the peaks become broader. This broadening suggests a significant refinement in the crystalline size. The similar phase formation of perovskite materials was observed in earlier studies [18, 19].
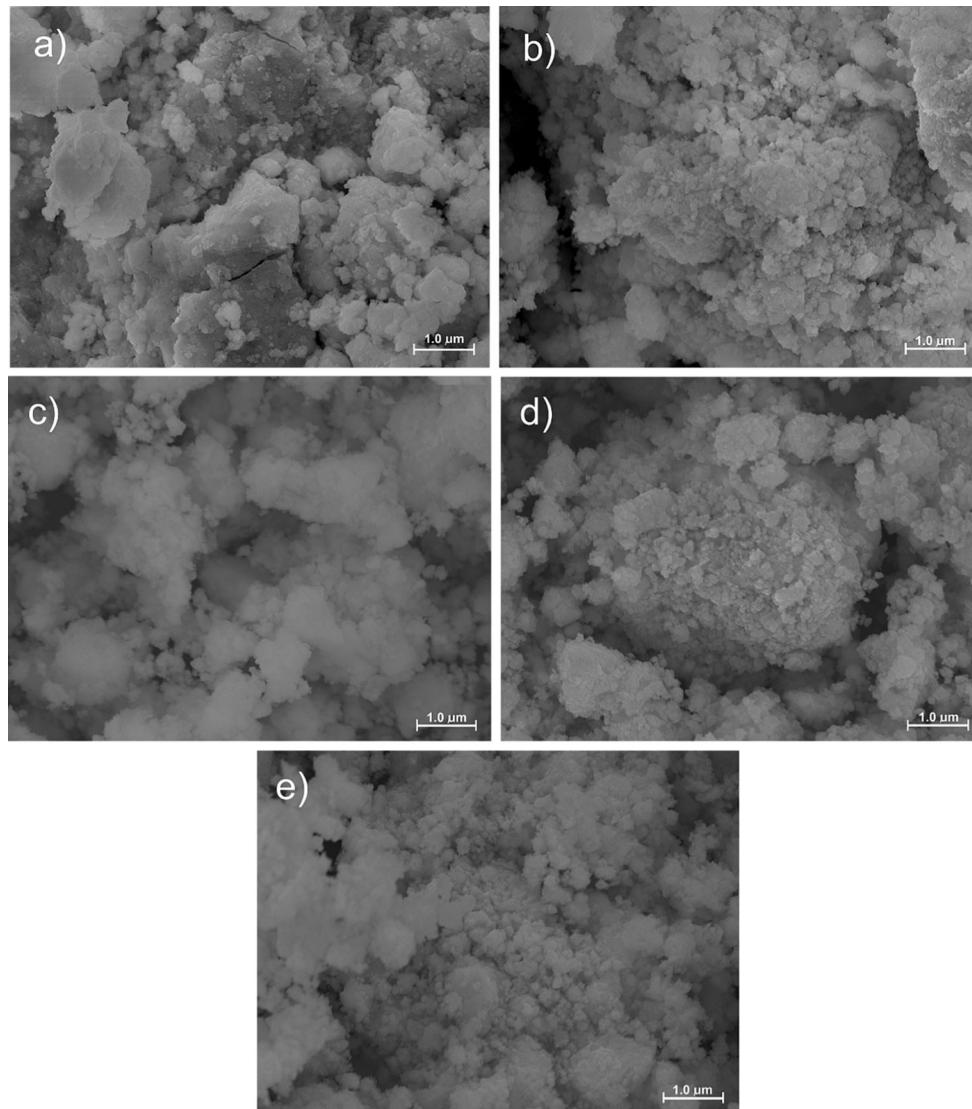
The main advantage of this route (the usage of oxides as substrates) is the direct formation of perovskite phase during mechanochemical treatment. Previously, [13] we have used carbonate as a starting reagent and consequently the calcination step was required to obtained perovskite phase.

The average crystal size of the powders can be estimated on the basis of XRD investigations and the Scherrer equation. The calculated average size of crystals slightly increases with increasing milling time, from 12 nm (for the powder milled for 10 h) to 20 nm (for the powder milled for 40 h). In case of the longer milling period (longer than 50 h), the average size gradually decreases up to 16 nm for the powder milled for 75 h.

The SEM images of the mechanochemically synthesized BFN powders, after different milling periods between 10 and 75 h, are presented in Fig. 2. High-energy milling incorporates large numbers of defects and crushes grains that enhance diffusion, consequently irregular and defected grains are formed. Those grains easily combine into loosely packed agglomerates. The lateral size of the agglomerates is relatively large, up to 40 μm. The performed investigation has not indicated any significant difference in morphology between the powders obtained after different milling periods.

The mechanochemically synthesized powders have been used for the preparation of the ceramic samples. The powders milled for a period shorter than 10 h, due to small amount of the perovskite phase, have not been used to obtain ceramic samples and for further investigation. The powder has been uniaxially pressed at room temperature and subsequent sintering at 1350 °C for 4 h. The density (ρ) of the BFN ceramics (measured by hydrostatic method) does not show a visible trend depending on the mixing time

Figure 1 XRD patterns of the started oxides and their mixture after different periods of high-energy milling.

Figure 2 SEM images of the BFN powders after high-energy milling for **a** 10 h, **b** 20 h, **c** 40 h, **d** 60 h and **e** 75 h.

Table 1 Parameters of the multiferroic BFN ceramics

|	BFN10h	BFN20h	BFN40h	BFN60h	BFN75h
ρ (g/cm^3)	6.11	6.13	5.85	5.93	6.06
d (µm)	11.6	12.8	12.3	13.5	14.7
T_m (°C)[a]	270	278	248	254	263
ε' at T_r[a]	47790	65280	18445	57588	62710
tanδ at T_r[a]	0.737	0.785	0.691	0.464	0.517
ε' at T_m[a]	136783	206365	65130	157475	157200
tanδ at 150 °C[a]	0.163	0.159	0.201	0.193	0.167
E_{Act} at I (eV)	0.539	0.514	0.638	0.454	0.4670
E_{Act} at II (eV)	0.917	0.900	0.837	0.811	0.750
ρ_{DC} at T_r (Ωm)	1.07×10^6	2.27×10^5	7.18×10^6	0.89×10^5	1.02×10^5

[a]Results for 1 kHz

ρ density, d the average grain size, T_r room temperature, T_m temperature at which there is maximum value of the dielectric permittivity, ρ_{DC} DC resistivity

(Table 1). This may be due to the random formation of powder agglomerates with different sizes.

The fracture of the BFN samples occurs through the grains, with a smooth topography of the surface, which indicates a higher mechanical strength of the interior of the grain (Fig. 3). Also the pores of the samples are visible on the morphology images. Such type of BFN ceramic morphology was observed early [15, 20]. The duration of high-energy milling affects the homogeneity of the BFN powders and, as a consequence, the ceramic morphology. The ceramics obtained from the powders after the shortest milling time (e.g., 10 h) exhibit a considerable non-uniformity of the shape and size of grains (with small and large grains), as well as large porosity. The increasing duration of high-energy milling improves the sinterability of powders and, as a result, reduces the porosity of the ceramic samples. Morphology of the BFN ceramics with the highest homogeneity occurs for the BFN60h sample, which indicates that the optimal time of high-energy milling is 60 h. The further continuation of the milling has not improved the ceramic morphology. The milling time of more than 60 h has induced the larger numbers of defects that consequently promote the formation of bigger grains (BFN75h sample). The average grain size (d) determined by the lineal intercept method of the BFN samples is summarized in Table 1.
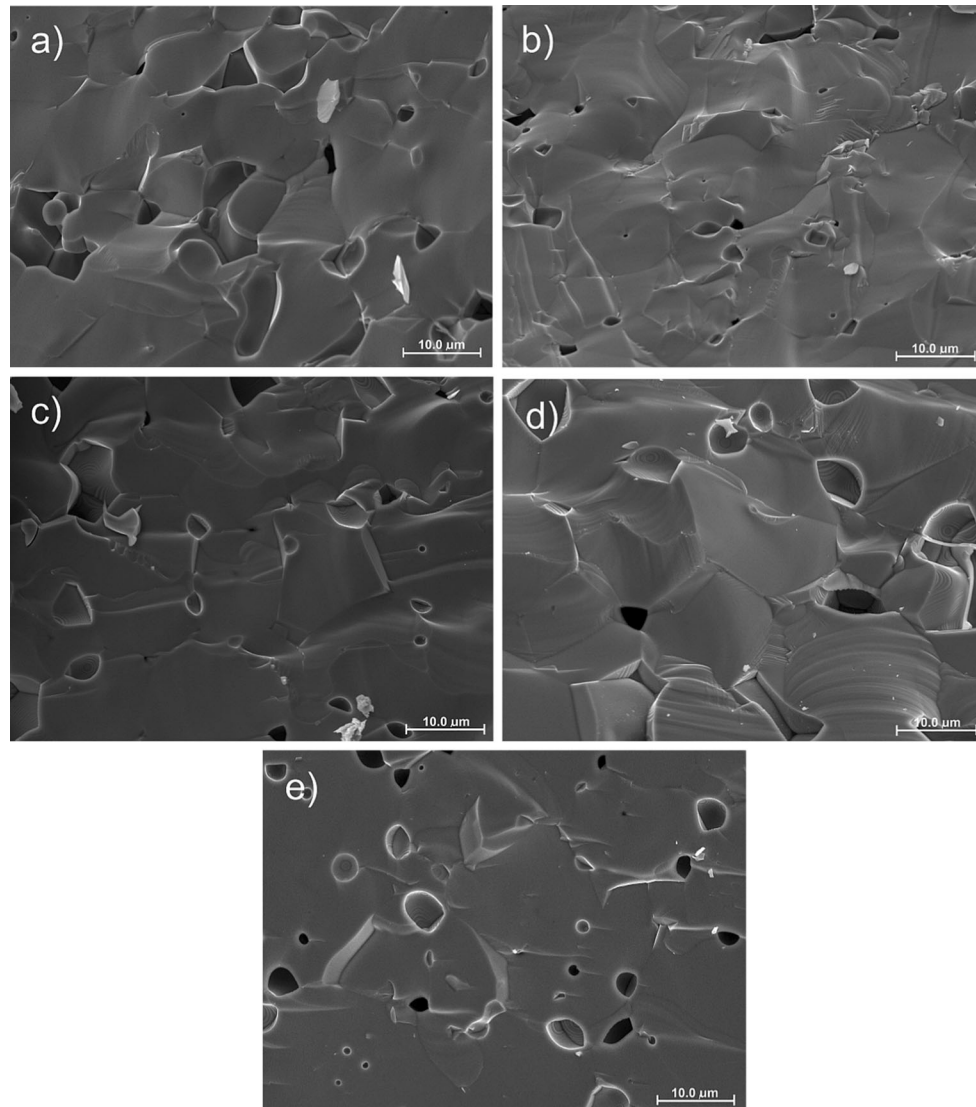
Figure 3 SEM microstructures of the BFN ceramics obtained from **a** 10-h, **b** 20-h, **c** 40-h, **d** 60-h and **e** 75-h high-energy-milled powders.
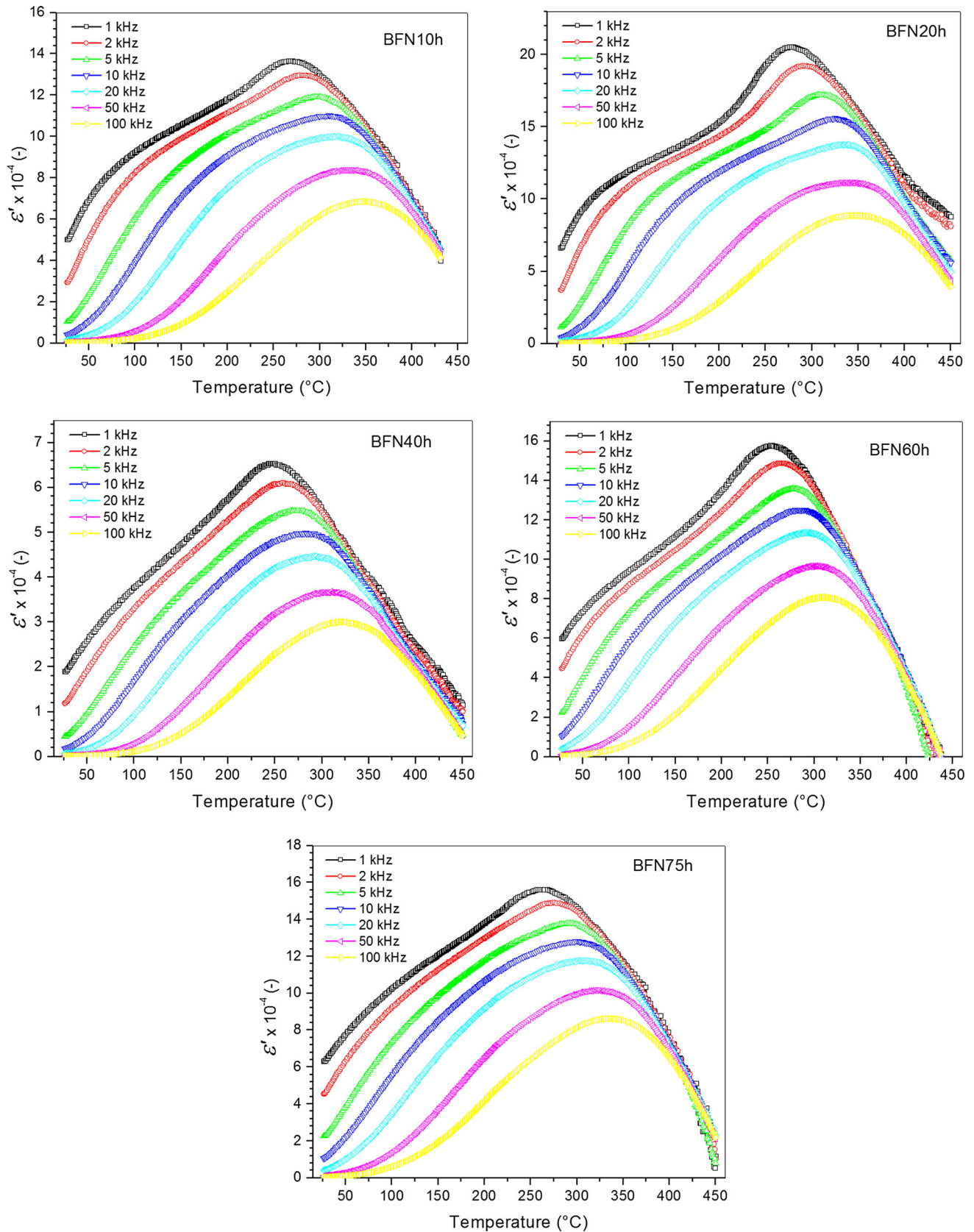
◄**Figure 4** Temperature dependencies of real dielectric permittivity (ε') measured during heating of BFN ceramics obtained from high-energy-milled powders.

The results of the temperature measurements of dielectric properties for different frequencies are presented in Figs. 4 and 5. In comparison with the work [17, 21], the $\varepsilon'(T)$ plots of the BFN ceramic samples show explicitly the phase transition for all measuring frequencies. The temperature of the $\varepsilon'(T)$ maximum (i.e., T_m) has shown a strong frequency dependence, whereas its value shifts to higher temperature with the frequency increasing.

For all BFN ceramic samples, the real dielectric permittivity increases during heating until it reaches diffuse maximum value of T_m connected with phase transition from ferroelectric to paraelectric phase. Such broad temperature range of the phase transition can be related to the disorder in the distribution of B-side ions in the unit cell. It leads to the formation of random local regions that exhibit different Curie temperatures. Such features, characteristic for the relaxor-like materials, have been observed in the perovskite materials [22]. The dielectric behaviors of the relaxor-like materials are in contrast to the normal ferroelectrics that exhibit a sharp, frequency-independent peak of $\varepsilon'(T)$ at the Curie temperature (T_C), e.g., observed in multicomponent PZT-type ceramics [23].

The real dielectric permittivity of the ceramics, prepared from mechanically synthesized powder, is characterized at room temperature by an extremely high value. Such giant value of dielectric permittivity [15, 22, 24] may be connected with a possibility of a layer (a metal–semiconductor layer) formation in the area near electrodes. The values of the dielectric permittivity calculated from the capacitance of such a two-layer capacitor are a sum of the sample capacitance and capacitance of the layers formed near the electrodes. The capacitance of such layers depends on the value of the blocking voltage and the amplitude of the electric field, and it influences the total dielectric permittivity values [25, 26]. The milling time dependence of real dielectric permittivity value is not clear; however, it is obvious that samples milled for a longer time have insignificant higher ε' at room temperature (Table 1). The BFN ceramics, prepared by the conventional process, reveal the phase transition in a narrower temperature range with high

values of dielectric permittivity [15]. However, compared to the present investigation, the values of dielectric permittivity at room temperature of the conventionally obtained BFN samples are lower [15, 17, 27].

The $\tan\delta(T)$ dependences of the all BFN ceramic samples show similar appearance (Fig. 5). Compared to the samples obtained by conventional solid-state reaction technique [15], the investigated BFN ceramics show much lower dielectric loss. With increasing temperature, the value of dielectric loss decreases just above the room temperature. In the temperature range of 130 °C–160 °C, the minimum value of dielectric loss of the BFN ceramics is observed. Above this temperature range, the rapid increase in the dielectric loss occurs, due to the increase in the electrical conductivity. For the BFN ceramics, similarly to the others perovskite-like materials, the losses in the ferroelectric phase are associated with re-polarization, whereas in the paraelectric phase with electric conduction [26]. This rapid growth of dielectric loss (in paraelectric phase) can be associated also with others factors, like a partial reduction of ions Fe^{3+}/Fe^{2+} or the formation of oxygen vacancies during sintering [28]. For higher frequencies, the values of the dielectric loss in the BFN samples increase.

The set of dielectric studies of the BFN ceramics, for 1 kHz, is presented in Fig. 6. Both the real dielectric permittivity values and the phase transition temperature depend on the high-energy milling time; nevertheless, this trend is not well established. On the other hand, the dielectric measurements of the BFN ceramic samples have not shown any significantly effect of the high-energy milling duration on dielectric loss values; however, the values of dielectric loss are lower compared to the works [17, 29].

The parameters of the dielectric dispersions, characteristic for the relaxor behavior, are collected in Table 2 for all BFN ceramics. The value of T_m strongly depends on the frequencies of the measuring electric field. The temperature dispersion between T_m observed at 1 kHz and 100 kHz changes with the high-energy milling duration. The smallest temperature dispersion (60 °C) is observed for the BFN60h ceramics obtained from 60-h-milled powder, while the larger one (81 °C) is observed for the BFN10h sample.

Figure 7 shows the frequency dependence of the real dielectric permittivity ε' and imaginary dielectric permittivity ε' for temperature range between 25 and
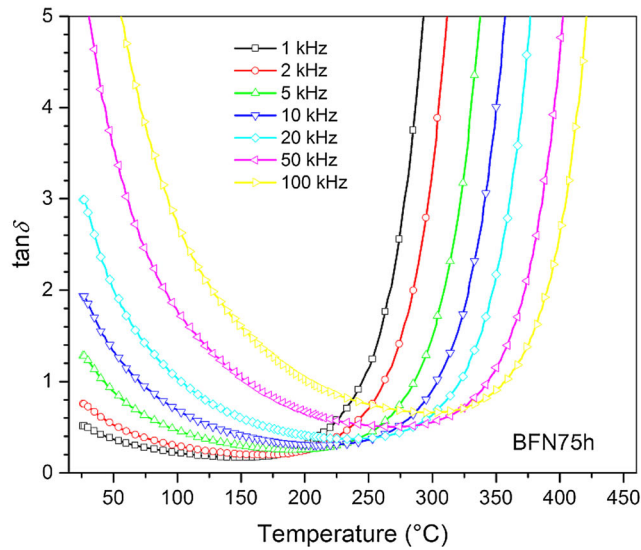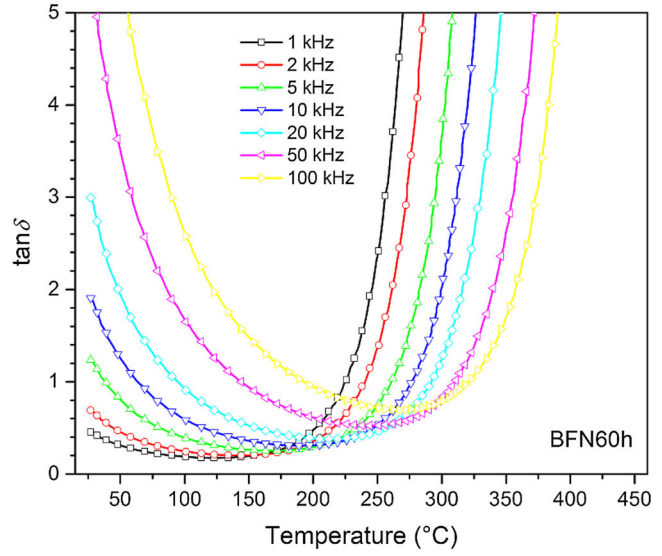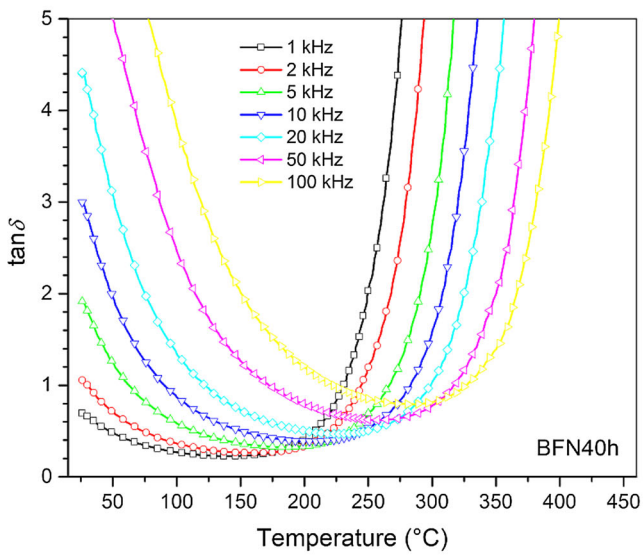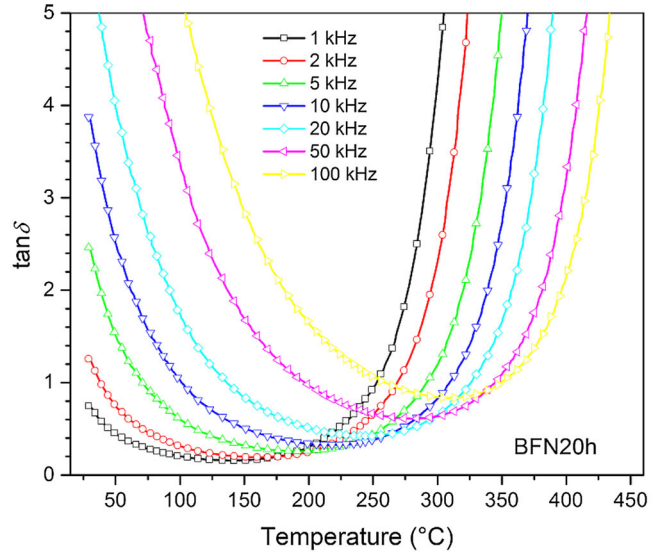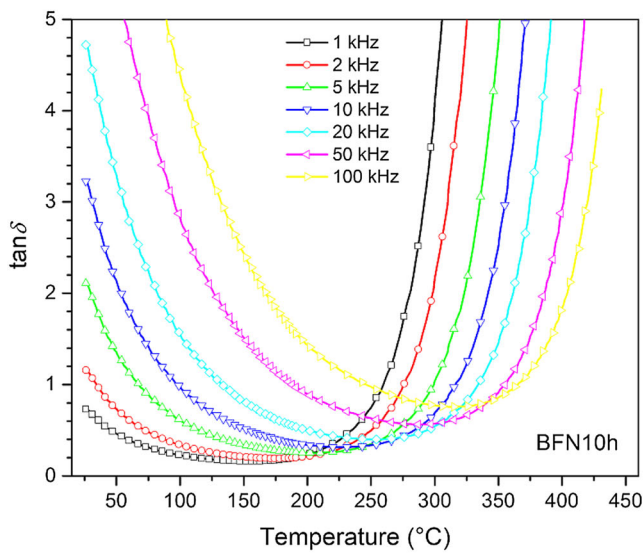
◄**Figure 5** Temperature dependencies of dielectric loss tanδ(T) measured during heating of BFN ceramics obtained from high-energy-milled powders.

400 °C. The inverse dependence on frequency has been observed for both ε' and ε'. Such behavior is typical for Debye-like relaxation and is related to the fact that dipoles can no longer follow the field at high frequencies (in low-frequency region the ionic polarizability dominant, while in the high-frequency region the effect of electronic polarizability is prevailing). Similar results were obtained for other lead-free perovskites like conventionally prepared BFN, BaFe$_{1/2}$Ta$_{1/2}$O$_3$ [14, 27].

Temperature measurements of DC electric conductivity of the BFN ceramics have not shown a clear trend of the effect of high-energy milling time on the σ_{DC} value. The differences in the DC conductivity values at the measurement range are small for all samples (Fig. 8). The lowest electrical conductivity has been measured for the BFN40h sample, while the highest conductivity—for the BFN75h sample. The values of activation energy E_{Act} below (I area) and above (II area) the phase transition temperature are summarized in Table 1. The higher values of the energy activation are observed for BFN ceramics obtained from the shorter milled powder. Also the results show that higher activation energy values occur for high temperatures, which is characteristic for materials with perovskite-like structure. In com-
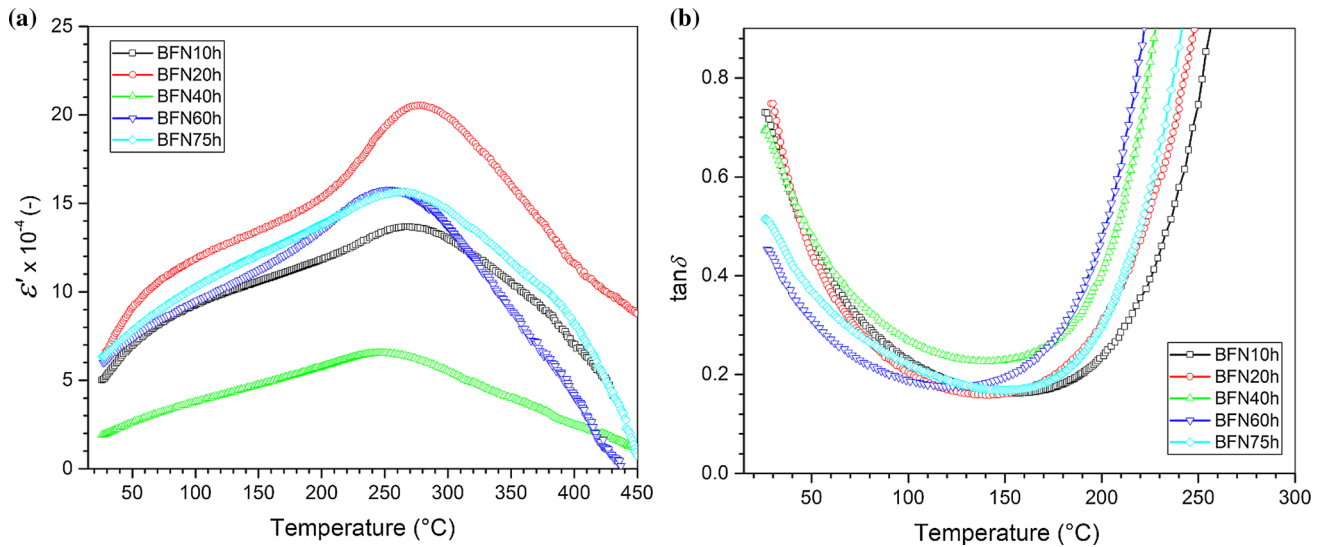

Figure 6 Dielectric properties of BFN ceramics obtained from 10-, 20-, 40-, 60- and 75-h-milled powders (measured at 1 kHz).

Table 2 T_m values obtained during heating for different samples and different measuring field frequencies of BFN ceramics

Frequency	T_m—temperature of the maximum of dielectric permittivity				
	BFN10h (°C)	BFN20h (°C)	BFN40h (°C)	BFN60h (°C)	BFN75h (°C)
1 kHz	270	278	248	254	263
2 kHz	282	293	260	266	278
5 kHz	299	313	276	280	294
10 kHz	310	326	285	288	302
20 kHz	318	338	297	294	309
50 kHz	336	347	314	304	326
100 kHz	351	353	326	314	339
ΔT (°C)	81	75	78	60	76

ΔT difference of temperature obtained for the highest (100 kHz) and the lowest frequency (1 kHz)
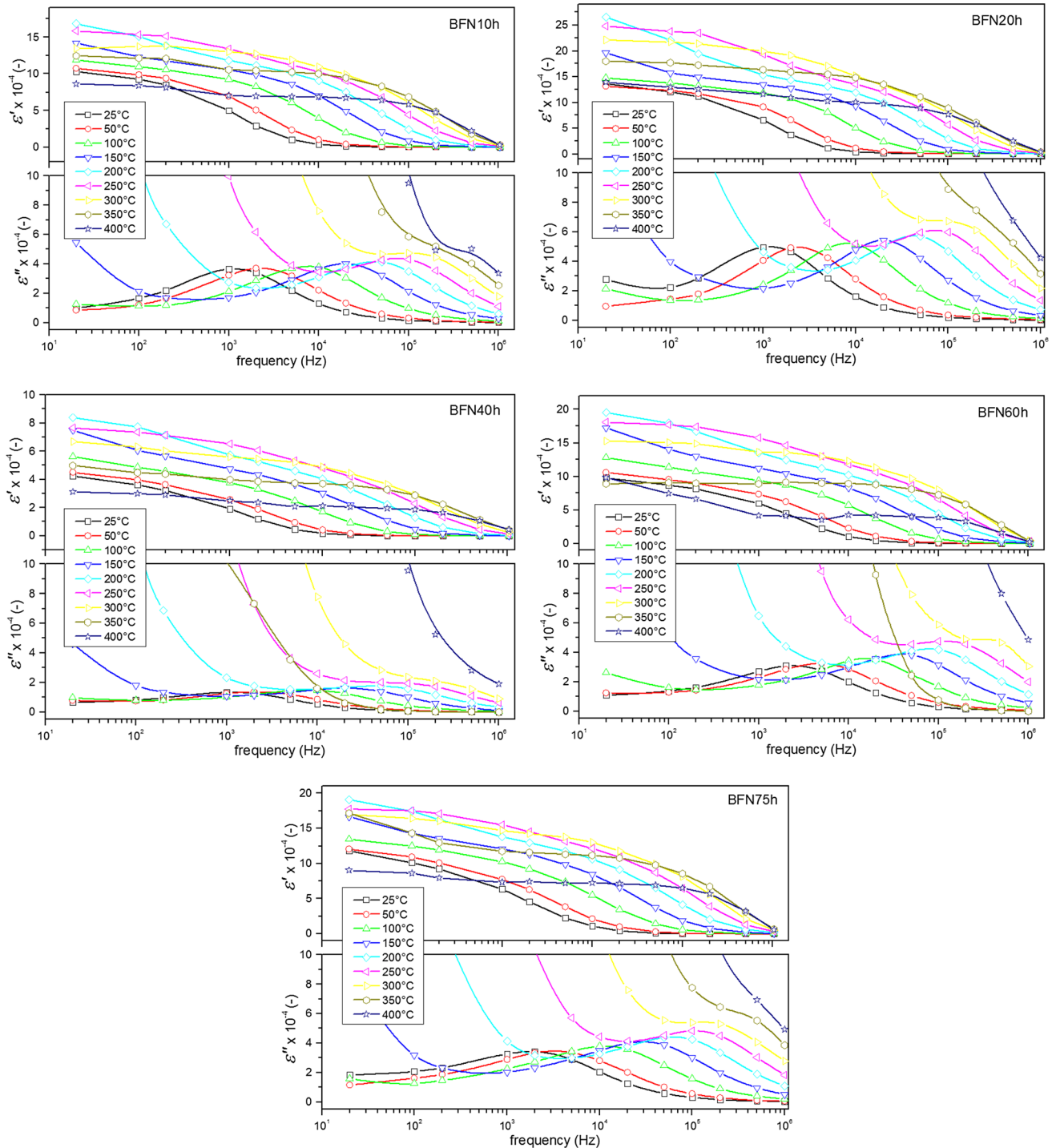
Figure 7 Frequency dependence of dielectric permittivity ε' and ε' for BFN ceramics in different temperature ranges.

parison with the BFN samples obtained in conventional method [15], the BFN samples obtained by mechanochemical method have lower resistance at room temperature, as well as have higher values of E_{Act} in paraelectric phase, and lower in ferroelectric one.

Conclusion

The multiferroic lead-free BFN ceramics have been successfully synthesized by mechanochemical method from the simple oxides. The first traces of perovskite phase have been observed after 2 h of
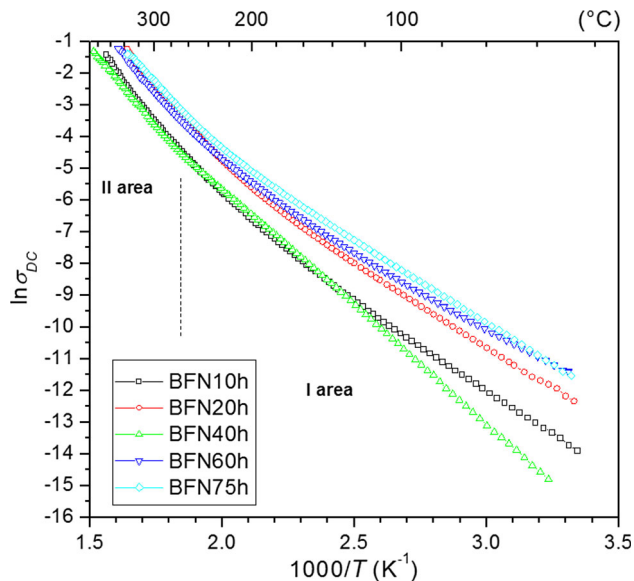
Figure 8 Lnσ_{DC} (1000/T) relationship of the BFN ceramics obtained from 10-, 20-, 25-, 40-, 60- and 75-h-milled powders.

high-energy milling (in the SPEX 8000 Mixer Mill; with BPR 5:1). The presented investigations have shown that the morphology of the BFN ceramic samples strongly depends on high-energy milling duration. High-energy milling process has also strongly affected the final properties of the ceramic samples. The influence of the high-energy milling duration on values of dielectric loss and dielectric permittivity, including the ferroelectric-paraelectric phase transition, has been observed. The values of the dielectric permittivity at room temperature are higher compared to BFN ceramics obtained by conventional methods. In comparison with the conventional BFN, the ceramics obtained from mechanically synthesized BFN powders exhibit lower dielectric loss. Considering the final parameters of the obtained ceramics, the optimal high-energy milling time is 60 h. From the application point of view, the usage of simple oxides as substrates and mechanochemical synthesis can shorten and simplify technological process (eliminated thermal treatment required for reaction initiation), as well as improve the parameters of the muliferroic BFN ceramics.

Acknowledgements

Compliance with ethical standards

Conflict of interest This contribution has been approved by all coauthors, it has not been published before, it is not under consideration for publication anywhere else, and there is no conflict of interest.

References

[1] Schmid H (2008) Some symmetry aspects of ferroics and single phase multiferroics. J Phys Condens Matter 20:434201. https://doi.org/10.1088/0953-8984/20/43/434201

[2] Kumar P (2011) Multiferroic materials and their properties. Integr Ferroelectr 131:25–35. https://doi.org/10.1080/10584587.2011.616397

[3] Picozzi S, Yamauchi K, Sergienko IA, Sen C, Sanyal B, Dagotto E (2008) Microscopic mechanisms for improper ferroelectricity in multiferroic perovskites: a theoretical review. J Phys Condens Matter 20:434208. https://doi.org/10.1088/0953-8984/20/43/434208

[4] Scott JF (2012) Applications of magnetoelectrics. J Mater Chem 22:4567–4574. https://doi.org/10.1039/C2JM16137K

[5] Wang KF, Liu J-M, Ren ZF (2009) Multiferroicity: the coupling between magnetic and polarization order. Adv Phys 58:321–448. https://doi.org/10.1080/00018730902920554

[6] Eerenstein W, Mathur ND, Scott JF (2006) Multiferroic and magneto electric materials. Nat Mater 442:759–765. https://doi.org/10.1038/nature05023

[7] Chu S-Y, Chen T-Y, Tsai I-T, Water W (2004) Doping effects of Nb additives on the piezoelectric and dielectric properties of PZT ceramics and its application on SAW device. Sensor Actuat A Phys 113:198–203. https://doi.org/10.1016/j.sna.2004.02.020

[8] Xiang P-H, Dong X-L, Chen H, Zhang Z, Guo J-K (2003) Mechanical and electrical properties of small amount of oxides reinforced PZT ceramics. Ceram Int 29:499–503. https://doi.org/10.1016/S0272-8842(02)00193-1

[9] Venkata Ramana M, Roopas Kiran S, Ramamanohar Reddy N, Siva Kumar KV, Murthy VRK, Murty BS (2011)

Investigation and characterization of Pb(Zr$_{0.52}$Ti$_{0.48}$)O$_3$ nanocrystalline ferroelectric ceramics: by conventional and microwave sintering methods. Mater Chem Phys 126:295–300. https://doi.org/10.1016/j.matchemphys.2010.11.023

[10] Raevski IP, Prosandeev SA, Bogatin AS, Malitskaya MA, Jastrabik L (2003) High dielectric permittivity in AFe$_{1/2}$B$_{1/2}$O$_3$ nonferroelectric perovskite ceramics (A = Ba, Sr, Ca; B = Nb, Ta, Sb). J Appl Phys 93:4130–4136. https://doi.org/10.1063/1.1558205

[11] Khim AS, Wang J, Junmin X (2000) Seeding effect in the formation of Pb(Fe$_{2/3}$W$_{1/3}$)O$_3$ via mechanical activation of mixed oxides. Solid State Ionics 132:55–61. https://doi.org/10.1016/S0167-2738(00)00689-5

[12] Xue JM, Wan DM, Wang J (2002) Functional ceramics of nanocrystallinity by mechanical activation. Solid State Ionics 151:403–412. https://doi.org/10.1016/S0167-2738(02)00546-5

[13] Bochenek D, Niemiec P, Szafraniak-Wiza I, Adamczyk M, Skulski R (2015) Preparation and dielectric properties of the lead-free BaFe$_{1/2}$Nb$_{1/2}$O$_3$ ceramics obtained from mechanically triggered powder. Eur Phys J B 88:277. https://doi.org/10.1140/epjb/e2015-60460-3

[14] Kar SK, Swain S, Sonia Kumar P (2015) High dielectric constant and low optical band gap studies of La-modified Ba(Fe$_{0.5}$Nb$_{0.5}$)O$_3$ ceramics. Mater Chem Phys 155:171–177. https://doi.org/10.1016/j.matchemphys.2015.02.021

[15] Bochenek D, Surowiak Z, Poltierova-Vejpravova J (2009) Producing the lead-free BaFe$_{0.5}$Nb$_{0.5}$O$_3$ ceramics with multiferroic properties. J Alloys Compd 487:572–576. https://doi.org/10.1016/j.jallcom.2009.08.015

[16] Eitssayeam S, Intatha U, Pengpat K, Rujijanagul G, MacKenzie KJD, Tunkasiri T (2009) Effect of the solid-state synthesis parameters on the physical and electronic properties of perovskite-type Ba(Fe, Nb)$_{0.5}$O$_3$ ceramics. Curr Appl Phys 9:993–996. https://doi.org/10.1016/j.cap.2008.10.003

[17] Eitssayeam S, Intatha U, Pengpat K, Tunkasiri T (2006) Preparation and characterization of barium iron niobate (BaFe$_{0.5}$Nb$_{0.5}$O$_3$) ceramics. Curr Appl Phys 6:316–318. https://doi.org/10.1016/j.cap.2005.11.008

[18] Szafraniak I, Hilczer B, Pietraszko A, Talik E (2008) Phase formations during mechanochemical synthesis of PbTiO$_3$. J Electroceram 20:21–25. https://doi.org/10.1007/s10832-007-9339-4

[19] Szafraniak-Wiza I, Kozielski L, Sebastian T (2016) Preparation and properties of Ba$_{1-x}$Ca$_x$TiO$_3$ nanopowders obtained by mechanochemical synthesis. Phase Transit 89:803–807. https://doi.org/10.1080/01411594.2016.1198962

[20] Bochenek D, Niemiec P, Chrobak A, Ziółkowski G, Błachowski A (2014) Magnetic and electric properties of the lead free ceramic composite based on the BFN and ferrite powders. Mater Charact 87:36–44. https://doi.org/10.1016/j.matchar.2013.10.027

[21] Sonia Chandrasekhar M, Kumar P (2017) Microwave assisted sol-gel synthesis of high dielectric constant CCTO and BFN ceramics for MLC applications. Process Appl Ceram 11:154–159. https://doi.org/10.2298/PAC1702154C

[22] Bochenek D, Zachariasz R (2009) PFN ceramics synthesized by a two-stage method. Arch Metall Mater 54:903–910

[23] Bochenek D, Zachariasz R (2015) Structure and physical properties of PZT-type ceramics with cadmium and tungsten dopants. Phase Transit 88:799–810. https://doi.org/10.1080/01411594.2014.992897

[24] Intatha U, Eittssayeam S, Wang J, Tunkasiri T (2010) Impedance study of giant dielectric permittivity in BaFe$_{0.5}$Nb$_{0.5}$O$_3$ perovskite ceramic. Curr Appl Phys 10:21–25. https://doi.org/10.1016/j.cap.2009.04.006

[25] Wójcik K, Zieleniec K, Milata M (2003) Electrical properties of lead iron niobate PFN. Ferroelectrics 289:107–120. https://doi.org/10.1080/00150190390221331

[26] Bochenek D, Surowiak Z (2009) Applications of iron (III) nitrate to obtain the multiferroic Pb(Fe$_{1/2}$Nb$_{1/2}$)O$_3$ ceramics by the sol–gel method. J Alloys Compd 480:732–736. https://doi.org/10.1016/j.jallcom.2009.02.045

[27] Mahto UK, Roy SK, Chaudhuri S, Prasad K (2016) Effect of milling on the electrical properties of Ba(Fe$_{1/2}$Ta$_{1/2}$)O$_3$ ceramic. Adv Mater Res 5:181–192. https://doi.org/10.12989/amr.2016.5.3.181

[28] Fang B, Shan Y, Tezuka K, Imoto H (2006) Phase formation, microstructure and physical properties of lead iron scandium niobate. J Eur Ceram Soc 26:867–873. https://doi.org/10.1016/j.jeurceramsoc.2004.11.020

[29] Ke S, Fan H, Huang H (2009) Dielectric relaxation in A$_2$FeNbO$_6$ (A = Ba, Sr, and Ca) perovskite ceramics. J Electroceram 22:252–256. https://doi.org/10.1007/s10832-007-9353-6